

# Hybrid model of GeV-TeV gamma ray emission from Galactic Center

Yi-Qing Guo<sup>1</sup>, Qiang Yuan<sup>1,2</sup>, Cheng Liu<sup>1</sup>, Ai-Feng Li<sup>3</sup>

<sup>1</sup>Key Laboratory of Particle Astrophysics, Institute of High Energy Physics, Chinese Academy of Science, Beijing 100049, P. R. China

<sup>2</sup>Key Laboratory of Dark Matter and Space Astronomy, Purple Mountain Observatory, Chinese Academy of Sciences, Nanjing 210008, P. R. China

<sup>3</sup> School of Information Science and Engineering, Shandong Agriculture University, Taian ,271018, China

E-mail: yuanq@ihep.ac.cn

**Abstract.** The observations of high energy  $\gamma$ -ray emission from the Galactic center (GC) by HESS, and recently by Fermi, suggest the cosmic ray acceleration in the GC and possibly around the supermassive black hole. In this work we propose a lepton-hadron hybrid model to explain simultaneously the GeV-TeV  $\gamma$ -ray emission. Both electrons and hadronic cosmic rays were accelerated during the past activity of the GC. Then these particles would diffuse outwards and interact with the interstellar gas and background radiation field. The collisions between hadronic cosmic rays with gas is responsible to the TeV  $\gamma$ -ray emission detected by HESS. With fast cooling in the strong radiation field, the electrons would cool down and radiate GeV photons through inverse Compton scattering off the soft background photons. This scenario provides a natural explanation of the observed GeV-TeV spectral shape of  $\gamma$ -rays.

## 1. Introduction

It is well known that the Galactic center (GC) region has a very complex astrophysical environment and is rich in various kinds of objects, and is a good library for the study of astrophysical phenomena. A supermassive black hole with mass  $\sim 4 \times 10^6 M_\odot$ , Sgr A\*, lies in the GC. Although the GC is rather quiet nowadays, frequent flares were observed in the X-ray as well as near infrared (NIR) bands [1, 2, 3], which means the existence of continuous weak activities of the black hole.

As a consequence high energy particles could be accelerated during such kinds of activities and imprinted in the  $\gamma$ -ray sky. The very high energy (VHE)  $\gamma$ -rays from the GC have been observed by several atmospheric Cerenkov telescopes such as CANGAROO [4], VERITAS [5], HESS [6, 7, 8], and MAGIC [9]. Recently GeV  $\gamma$ -ray emission from the GC was also revealed by the spatial detector Fermi Large Area Telescope (Fermi-LAT, [10]). The observations in both TeV and GeV bands showed that the  $\gamma$ -ray emission tended to be stable without significant variability [8, 9, 10].

Several models have been proposed to explain the  $\gamma$ -ray emission observed at the GC, including hadronic models [11, 12, 13, 10, 14, 15] and leptonic ones [16, 17]. An issue prevents a simple explanation to the GeV-TeV spectra of the GC is that the GeV  $\gamma$ -ray emission is not consistent with the direct extrapolation of TeV  $\gamma$ -rays to the low energy range. Chernyakova et al. [10] proposed that the strong energy dependence of the diffusion coefficient would separate the low energy and high energy particles into two different diffusion regimes and the GeV-TeV spectral shape of the  $\gamma$ -rays could be reproduced. In [15] the stochastic acceleration of particles in a two-phase interstellar medium (ISM) was employed to generate two distinct populations of protons to explain the data. In [17] the Fermi-LAT  $\gamma$ -ray emission was suggested to originate from a population of electrons ICS off the soft background photons and the VHE  $\gamma$ -ray emission was thought to be from different sources instead of Sgr A\*.

The morphology study of the VHE  $\gamma$ -ray source, HESS J1745-290, by HESS showed no spatial extension and the upper limit of the angular size of  $\sim 1'.3$  was set [18]. Note there is another diffuse component of the  $\gamma$ -ray emission along the ridge [19, 20], which is not discussed in this work. It may imply that the high energy particles are confined in several parsec regions around the GC [10, 15] or the high concentration of the target gas in the inner region [14].

In this work, we propose a hybrid model to explain the GeV and TeV  $\gamma$ -ray emission. It is natural to expect that both protons and electrons can be accelerated during the GC activity. Therefore without finely tuning the environmental parameters, we should expect the existence of two components of the  $\gamma$ -ray emission, which is just the case shown by the GeV-TeV observations. A simple expectation is that high energy protons interact with the ISM is responsible to the VHE  $\gamma$ -rays, and the electrons, which may cool down in the GC radiation field and/or magnetic field, produce the GeV  $\gamma$ -rays through inverse Compton scattering (ICS) off the background photons. In Sec. 2, we present the detailed modeling of this picture. Sec. 3 is the discussion and the main

conclusions are summarized in Sec. 4.

## 2. Model and results

Although the overall behavior of Sgr A\* is quite silent, the observations in X-ray and infrared bands indicate that it still has continuous weak activities [21, 22, 1, 2]. During such kinds of activities, the accretion of stars and gas by the supermassive black hole could be effective to accelerate particles. We assume that both the protons and electrons were accelerated instantaneously during such flare events. Then these particles would diffuse away from the acceleration site, and radiate during the propagation. The propagation equation for both protons and electrons can be written as

$$\frac{\partial \phi}{\partial t} = \frac{D(E)}{r^2} \frac{\partial}{\partial r} r^2 \frac{\partial \phi}{\partial r} + \frac{\partial}{\partial E} [b(E)\phi] + N(E)\delta(t)\delta(\mathbf{r}), \quad (1)$$

where  $\phi(r, E, t)$  is the propagated flux as a function of space, energy and time,  $D(E)$  is the diffusion coefficient,  $N(E)$  is the injection spectrum of particles at  $t = 0$  and  $\mathbf{r} = 0$ , and  $b(E) \equiv dE/dt$  is the energy loss rate, which is important for electrons but negligible for protons. The energy dependence of diffusion coefficient is assumed to be power-law of rigidity  $R$ ,  $D(R(E)) = \beta D_0(R/4 \text{ GV})^\delta$ , in which  $\delta$  is the spectral index and  $\beta$  is the particle velocity. In this work we assume  $\delta = 0.3$ , which is close to a Kolmogorov type of the ISM turbulence.

The solution of the above equation for electrons is [23]

$$\phi_e(r, E, t) = \frac{N_e(E_i)b(E_i)}{\pi^{3/2}b(E)r_{\text{dif}}^3} \exp\left(-\frac{r^2}{r_{\text{dif}}^2}\right), \quad (2)$$

where  $E_i$  is the initial energy of the electron whose energy is cooled down to  $E$  at time  $t$ , and  $r_{\text{dif}}(E, t) = 2\sqrt{\Delta u}$ , in which

$$\Delta u(E, E_i) = \int_E^{E_i} \frac{D(E')}{b(E')} dE', \quad (3)$$

is the effective diffusion length when the particle energy decreases from  $E_i$  to  $E$ .

For protons we neglect the energy loss term, and the solution of the propagation equation is even simpler

$$\phi_p(r, E, t) = \frac{N_p(E)}{(\sqrt{2\pi}\sigma)^3} \exp\left(-\frac{r^2}{2\sigma^2}\right), \quad (4)$$

where  $\sigma(E, t) = \sqrt{2D(E)t}$  is the effective diffusion length within  $t$ .

The energy loss of electrons includes ICS off the soft background photons, synchrotron radiation in the magnetic field and bremsstrahlung radiation in the ISM. The soft photons consist with infrared from dust and optical from stars. In [22] the measurement of infrared emission in the central 1.2 pc was presented. According to the data, the expected optical emission was proposed based on assumptions of the optical photon energy density [24, 16, 17]. Taking the uncertainties of the expected optical emission into account, we adopt the two models given in [24, 17] in this work. The

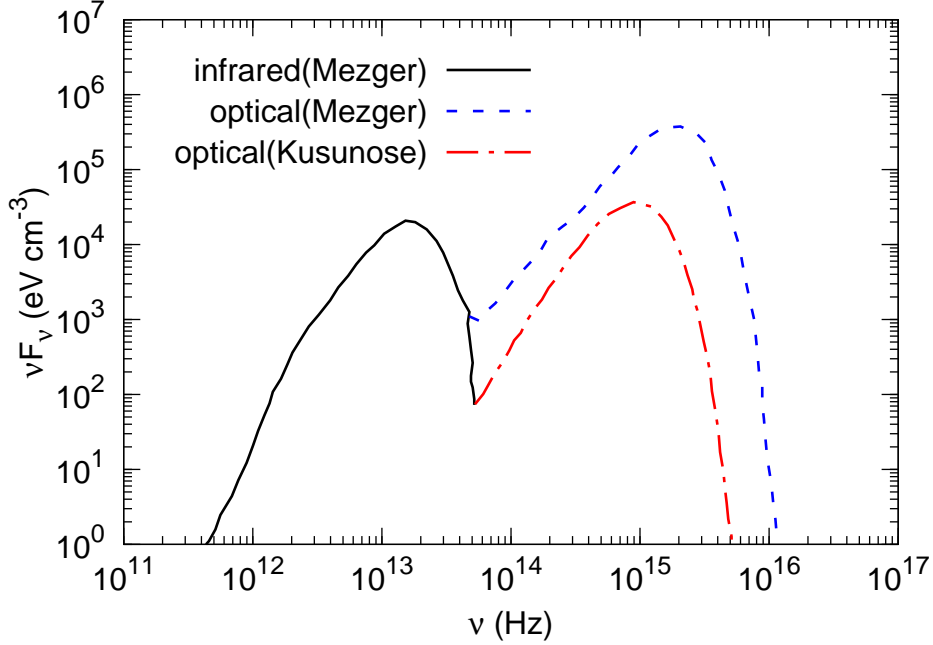


**Figure 1.** Infrared and optical photon energy density spectrum in  $\sim 1$  pc of the GC region. The solid line is adopted from [24] which is consistent with the observational data [22]. The dashed and dash-dotted lines are the model expected results of optical emission presented in [24] and [17] respectively. This figure is a reproduction of Fig. 1 in [17].

intensity of the soft photons is shown in Figure 1. The magnetic field strength varies with the radius away from the GC [25]. For the very small region ( $r \sim \text{pc}$ ) the average magnetic field strength is adopted to be  $\sim 10^2 \mu\text{G}$  [25, 17]. As for the ISM density, there is large uncertainty in the GC region. Typically the adopted ISM density within  $\sim \text{pc}$  region is of the order  $10^3 \text{ cm}^{-3}$  [10, 14]. Compared with the ICS energy loss in the strong radiation field, the bremsstrahlung energy loss is negligible [26].

We calculate the cooling time of the electrons,  $\tau = E/(dE/dt)$ , in the above background photons field and magnetic field, as shown in Figure 2. Here the optical emission is adopted to be the one of Kusunose & Takahara (2012) [17]. It is shown that the energy loss of electrons is dominated by the ICS up to  $> 10$  TeV.

In Figure 3 we show the integral spectra of both electrons and protons after time  $t$  of the injection. The integral radius is taken to be 1.2 pc for electrons and 3 pc for protons respectively. For electrons we integrate the particles within radius  $\sim 1.2$  pc since the high background photon density is expected to exist in that region, and most of the radiation should come from such a region. However, for protons, we adopt a some larger integral radius,  $\sim 3$  pc, according to the spatial extension upper limit of HESS J1745-290 derived by HESS [18]. The diffusion coefficient is  $D_0 = 10^{27} \text{ cm}^2 \text{ s}^{-1}$ , and the injection spectra of both electrons and protons are adopted as  $E^{-1.9}$ . We can see from this figure that the cooling of electrons will result in a cutoff of the spectrum, above which the electrons can not survive from the energy loss. The cutoff energy depends on the time.

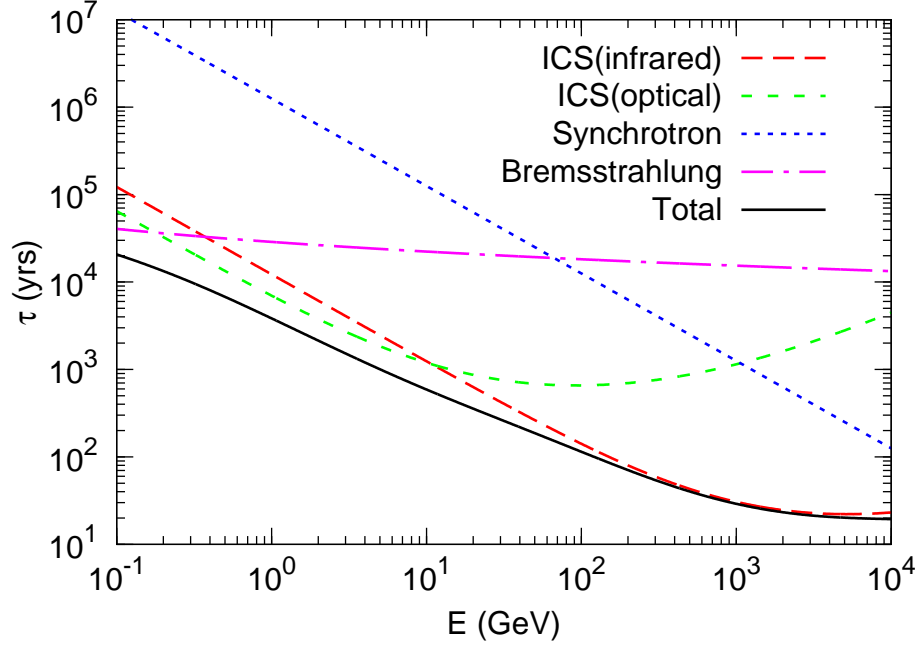


**Figure 2.** The cooling time of electrons in the background photon field model of Kusunose & Takahara (2012) [17] and magnetic field with  $B = 100\mu\text{G}$ . The ISM density is adopted to be  $10^3 \text{ cm}^{-3}$  to calculate the bremsstrahlung energy loss.

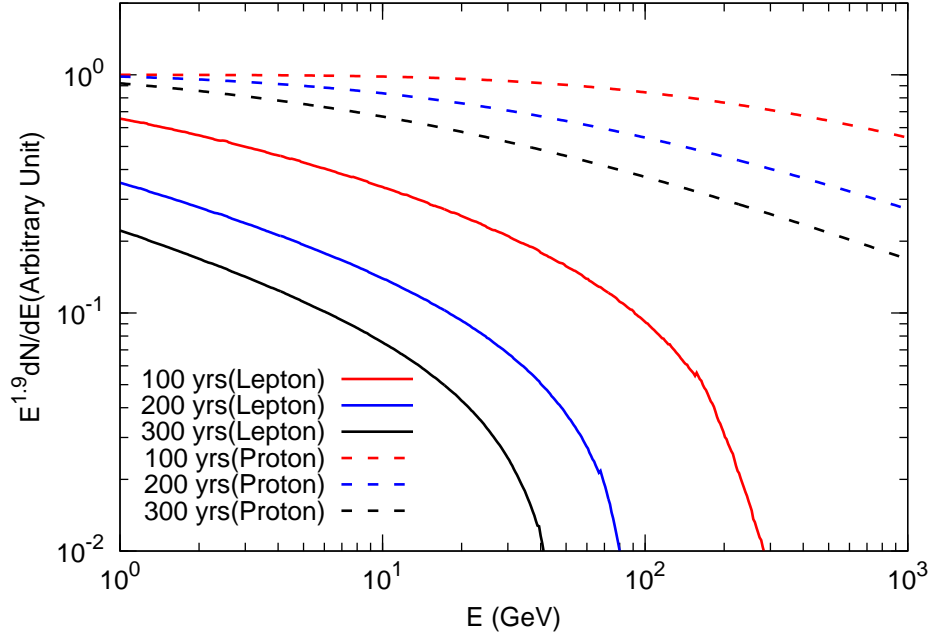


**Figure 3.** Propagated electron (solid) and proton (dashed) spectra for observational time  $t = 100, 200$  and  $300$  (from top to bottom) years respectively. The energy loss of electrons adopted in this calculation is shown in Figure 2.

The younger the injection is, the higher energy of electrons we can observe. The spectral shape also has an evolution with the time. For shorter time, the relative fraction of low

energy particles is smaller due to slower propagation of low energy particles, which results in harder spectra. For protons there is also a time evolution of the spectra. It reflects the fact that for longer time, more high energy particles will diffuse out of the integral region and result in a soft spectrum.

Then we discuss the  $\gamma$ -ray emission of those electrons and protons in the background radiation field and the interstellar medium. For electrons we consider only the ICS emission and neglect the bremsstrahlung radiation. The Klein-Nishina cross section of ICS is employed. For the  $\gamma$ -ray emission from  $pp$  collisions, we use the parameterization given in [27].

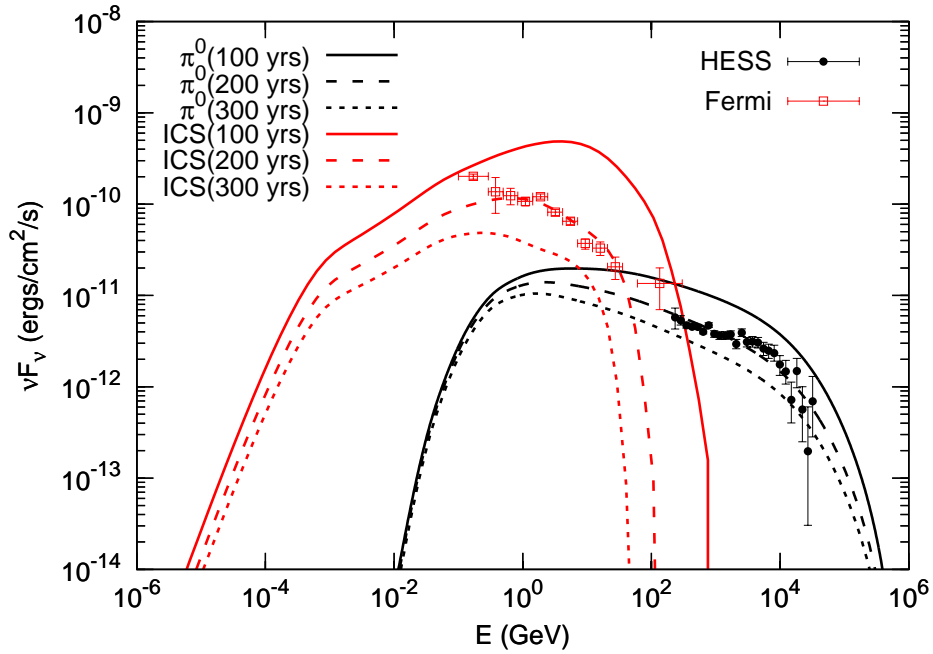


**Figure 4.** Calculated  $\gamma$ -ray spectra of the hybrid model, compared with the observational data by Fermi-LAT [10] and HESS [28]. Different lines show the effect of observational time  $t$  (100, 200 and 300 yr from top to bottom). The diffusion coefficient is  $D_0 = 10^{27} \text{ cm}^2 \text{ s}^{-1}$ . The soft background photon model is Kusunose & Takahara (2012) [17].

Figure 4 presents the results of the calculated  $\gamma$ -ray spectra and the comparison with the observational data [10, 28]. The injection spectra are adopted to be  $\propto E^{-1.9}$ , and the diffusion coefficient is adopted to be  $D_0 = 10^{27} \text{ cm}^2 \text{ s}^{-1}$ . The background photon model is adopted to be Kusunose & Takahara (2012) [17]. Three different observational time  $t = 100, 200$  and  $300$  yr are shown. The observational time determines the cutoff energy of the electron spectrum (see Figure 3). We find that for the Kusunose & Takahara (2012) photon field  $t \sim 200$  yr can match the data well $^\ddagger$ . Another effect of the time  $t$ , is the overall normalization. If  $t$  is larger, more particles diffuse out of the  $\sim \text{pc}$  region,

$^\ddagger$  Here we do not intend to fit the data to find the best parameters, but just to show the rough comparison between the model and data. Except the first data point of Fermi-LAT, we actually find rather good description to the data of the model (dashed line). There could be systematic uncertainty of

and we expect a decrease of the overall normalization of the integral particle spectra. For  $t = 200$  yr we find the total energy of electrons above 1 GeV is  $\sim 5 \times 10^{47}$  erg to match the Fermi-LAT data. The electron-to-proton ratio  $K_{ep}$  is about  $0.22(n/10^3 \text{ cm}^{-3})$  in this case. Note, however, a significant part of high energy protons ( $E > 10$  TeV) will diffuse out of the 3 pc region in this case, as can be seen from Figure 3. Therefore to be consistent with the morphology of the source, we may require the gas density is higher in inner 3 pc region than outside, as the scenario of [14].

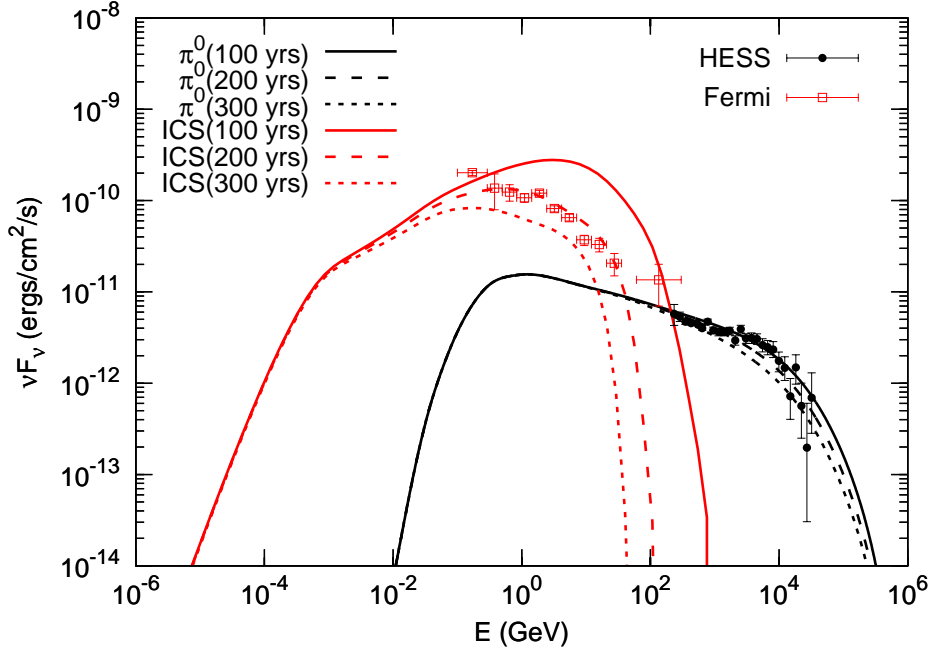


**Figure 5.** Same as Figure 4 but for smaller diffusion coefficient  $D_0 = 10^{26} \text{ cm}^2 \text{ s}^{-1}$ .

To be consistent with the cutoff behavior of VHE  $\gamma$ -rays observed by HESS, we employ an exponential cutoff of the proton spectrum with cutoff energy  $E_c = 200$  TeV. It is possible that the pair production of VHE photons in the background radiation field could also be responsible to the cutoff of the  $\gamma$ -ray spectra [29, 30]. However, our calculation shows that for the adopted soft background photon field in  $\sim$ pc region, the pair production attenuation is negligible. Thus the cutoff should be understood as the acceleration limit of the flaring event. The maximum energy protons can achieve for diffusive shock acceleration is [31]

$$E_{\text{max}} \sim eBR \approx 10^{21} \left( \frac{B}{\text{G}} \right) \left( \frac{R}{\text{pc}} \right) \text{ eV}, \quad (5)$$

where  $B$  is the magnetic field and  $R$  is the size of the acceleration region. As in [31], we assume the acceleration takes place within 10 Schwarzschild radii ( $R_g \sim 10^{12}$  cm) of the black hole. To accelerate protons to above 100 TeV requires a magnetic field  $\sim$ G

the data analysis of Fermi-LAT, especially at low energies, and adjusting properly the model parameters may also further improve the fit.

in the acceleration region. Such a condition could be reached in the very central region of the GC [31]. On the other hand, if the acceleration takes place in larger regions, the required magnetic field could be smaller.

Figure 5 shows the results for even smaller diffusion coefficient  $D_0 = 10^{26} \text{ cm}^2 \text{ s}^{-1}$ . In this case most of the protons up to 100 TeV may still be confined in several pc region around the GC. As a simple estimate, the diffusion length for protons is about  $1.8 \left( \frac{D_0}{10^{26} \text{ cm}^2 \text{ s}^{-1}} \right)^{0.5} \left( \frac{E}{100 \text{ TeV}} \right)^{0.15} \left( \frac{t}{200 \text{ yr}} \right)^{0.5} \text{ pc}$ . The accumulative spectrum of protons is similar with the injection spectrum. Therefore we adopt the injection spectrum  $\propto E^{-2.2}$  to be consistent with the HESS data. The results show a good fit to the GeV-TeV observational data for  $t = 200 \text{ yr}$  too. It is shown that for protons different time  $t$  leads to small differences of the results, which means that indeed most of the protons are confined. We also note that the differences of the ICS spectra with respect to  $t$  are larger than that of  $\pi^0$  decay spectra. This is simply because the integral radius of electrons is smaller than that of protons. The total energy of electrons above 1 GeV is  $\sim 8 \times 10^{46} \text{ erg}$  in this case, and the electron-to-proton ratio  $K_{ep}$  is  $0.05(n/10^3 \text{ cm}^{-3})$ .

Finally, the results for Mezger et al. (1996) soft background photon model [24] are shown in Figure 6. Other conditions are the same as Figure 4. Compared with Kusunose & Takahara (2012) photon field, the optical emission is stronger and the cooling time for electrons is shorter. Thus for  $t \sim 150 \text{ yr}$  the cutoff energy of electrons is proper to fit the Fermi-LAT data. However, the energy spectrum of ICS emission does not differ significantly from that shown in Figure 4. This is because in stronger background radiation field the cooling is more significant, and a larger cooling is just canceled out when calculating the ICS  $\gamma$ -ray spectrum in such a radiation field. The total energy of electrons above 1 GeV is  $\sim 1.6 \times 10^{47} \text{ erg}$ , and the electron-to-proton ratio  $K_{ep}$  is about  $0.11(n/10^3 \text{ cm}^{-3})$ .

### 3. Discussion

The diffusion coefficient adopted in this work is  $D_0 \sim 10^{26} - 10^{27} \text{ cm}^2 \text{ s}^{-1}$ , which is much smaller than that in the disk and halo ( $\sim 10^{28} - 10^{29}$  as induced from the cosmic ray transportation). This might be due to the higher magnetic field and more turbulent ISM in the GC region. The lower limit of the diffusion coefficient should be the Bohm limit, which is  $D_{\text{Bohm}} = pv/3eB \sim 3 \times 10^{25} (p/\text{TeV})(B/\mu\text{G})^{-1} \text{ cm}^2 \text{ s}^{-1}$  [32, 33, 34]. The diffusion coefficient adopted in this work is well larger than the Bohm limit in the whole energy range discussed.

In the calculation of proton propagation, the energy loss of protons via interaction with the ISM is neglected. As a rough estimate, the average collision probability of one projectile proton is about  $n\sigma v\tau \sim 0.01(n/10^3 \text{ cm}^{-3})(\tau/200 \text{ yr})$ . Thus for the typical parameters adopted in this work, the collisional energy loss of protons is indeed negligible.

The secondary electrons/positrons from charged pion decay due to  $pp$  collision could also contribute to the  $\gamma$ -ray emission. As a very rough estimate, for one  $pp$  collision,  $\gamma$ -ray photons will take 1/3 of the energy of all the pions, and  $e^\pm$  will take



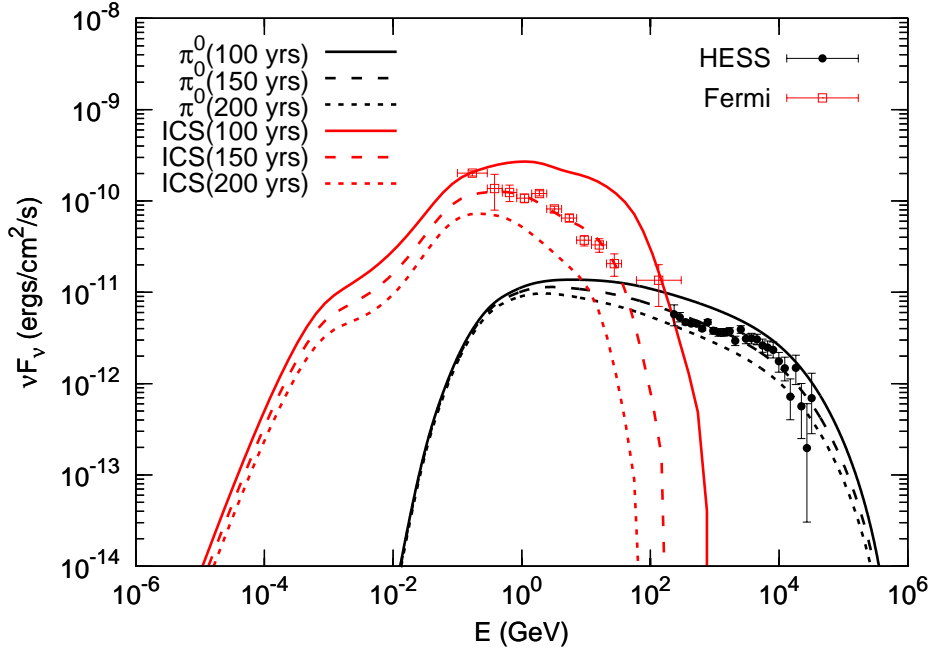


**Figure 6.** Same as Figure 4 but for the Mezger et al. (1996) soft background photon model [24].

$2/3 \times 1/3 = 2/9$  of the energy (assuming energy equipartition between  $e^\pm$  and neutrinos). Therefore the total energy of secondary  $e^\pm$  should be lower than that of  $\pi^0$  decaying  $\gamma$ -rays. Furthermore, the soft radiation field is restricted in 1.2 pc region around the black hole, while the  $pp$  collision occurs in  $\sim 3$  pc region. Therefore the contribution of the secondary  $e^\pm$  to the  $\gamma$ -rays through ICS emission should be much smaller than that of neutral pion decay.

The electron component will also produce synchrotron radiation in the magnetic field, and there might be constraints from the radio to X-ray data. As shown in [17] the synchrotron emission in  $\sim 100 \mu\text{G}$  magnetic field may exceed the radio measurement of Sgr A\* for the quiescent state [35]. However, the spatial scale of the present study is arc-minutes (pc), instead of arc-seconds as the radio observations show. The expected synchrotron emission is consistent with the data-based result of pc scale radio emission as given in [24].

Early in 2012, one bright flare of GC is observed by HETGS onboard of the Chandra X-ray observatory [3]. The total energy in 2 – 10 keV band was approximately  $10^{39}$  erg [3]. Assuming the total energy of this accretion event is about 4 orders of magnitude higher [24],  $\sim 10^{43}$  erg, and  $\sim 10\%$  of it converts to acceleration of cosmic rays, we give the expected  $\gamma$ -ray emission of such an event within the current framework of the model, as shown in Figure 7. The solid lines are same as that in Figure 4. The dashed line is the expected flux of the ICS emission, with the same parameters of the diffusion coefficients, injection spectral index and electron-to-proton ratio as that of Figure 4. The  $\gamma$ -ray emission at this stage is dominated by the ICS emission and the hadronic

component is much lower. We can see that the total flux of  $\gamma$ -rays is too low to be able to be detected by the current VHE  $\gamma$ -ray detectors. We should keep in mind that this estimate is very rough and suffers from large uncertainties of the assumption of total energy output of the flare and the energy fraction goes into particle acceleration. This gives us an impression that how large a flare is needed in order to produce the observed  $\gamma$ -rays.

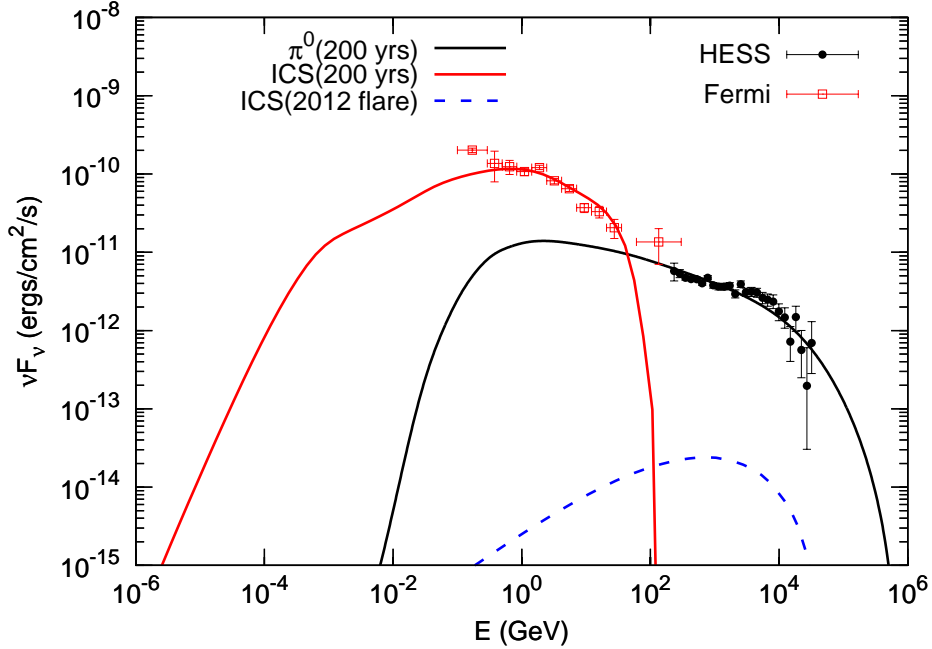


**Figure 7.** The expected  $\gamma$ -ray emission for the flare event of 2012. We assume the total power of the flare event is 4 orders of magnitude high than the 2 – 10 keV energy.

#### 4. Conclusion

In this work, a hybrid model is proposed to explain the GeV  $\gamma$ -ray emission observed by Fermi-LAT and TeV  $\gamma$ -ray emission observed by HESS telescope, of the GC. The current  $\gamma$ -ray emission could be originated from one flare with total energy  $\gtrsim 10^{48}$  ergs at  $\sim 10^2$  years ago. Both the protons and electrons were accelerated to very high energies in this flaring event. Furthermore the flaring event produced a thermal bath of soft photons in the GC region, with typical scale  $\sim \text{pc}$ . High energy particles could then diffuse out of the acceleration site and interact with the ambient medium and radiation fields. The hadronic collisions between protons and ISM gives rise to the TeV  $\gamma$ -rays. At the same time, electrons would lose energy through ICS and synchrotron radiation. The ICS photons could be responsible for the GeV  $\gamma$ -ray emission observed by Fermi-LAT.

## Acknowledgements

This work is supported by the Ministry of Science and Technology of China, Natural Sciences Foundation of China (Nos. 10725524, 10773011, 11135010 and 11105155), the Chinese Academy of Sciences (Nos. KJCX2-YW-N13, KJCX3-SYW-N2, GJHZ1004) and Natural Science Foundation of Shandong Province of China (ZR2009AM003). QY acknowledges the support from the Key Laboratory of Dark Matter and Space Astronomy of Chinese Academy of Sciences.

## References

- [1] Dodds-Eden, K., et al., 2009, ApJ, 698, 676
- [2] Dodds-Eden, K., et al., 2011, ApJ, 728, 37
- [3] Nowak, M. A., et al., 2012, ApJ, 759, 95
- [4] Tsuchiya, K., et al., 2004, ApJ, 606, 115
- [5] Kosack, K., et al., 2004, ApJ, 608, 97
- [6] Aharonian, F., et al., 2004, A&A, 425, 13
- [7] Aharonian, F., et al., 2006, Phys. Rev. Lett., 97, 9901
- [8] Aharonian, F., et al., 2008, A&A, 492, 25
- [9] Albert, J., 2006, ApJ, 638, 101
- [10] Chernyakova, M., et al., 2011, ApJ, 726, 60
- [11] Atoyan, A. & Dermer, C. D. 2004, ApJ, 617, L123
- [12] Liu, S., et al., 2006, ApJ, 647, 1099
- [13] Ballantyne, D. R., et al., 2007, ApJ, 657, L13
- [14] Linden, T., et al., 2012, ApJ, 753, 41
- [15] Fatuzzo, M. & Melia, F., 2012, ApJ, 757, L16
- [16] Hinton, J. A. & Aharonian, F. A., 2007, ApJ, 657, 302
- [17] Kusunose, K. & Takahara, F., 2012, ApJ, 748, 34
- [18] Acero, F., et al., 2010, MNRAS, 402, 1877A
- [19] Aharonian, F., et al., 2006, Nature, 439, 695
- [20] Yusef-Zadeh, F., et al., 2012, arXiv:1206.6882
- [21] Becklin, E. E., Gatley, I. & Werner, M. W., 1982, ApJ, 258, 135
- [22] Davidson, J. A., 1992, ApJ, 387, 189
- [23] Atoyan, A. M., Aharonian, F. A. & Volk, H. J., 1995, Phys. Rev. D, 52, 3265
- [24] Mezger, P. G., Duschl, W. J. & Zylka, R., 1996, A&AR, 7, 289
- [25] Bertone, G. et al., 2009, JCAP, 03, 009
- [26] Strong, A. W. & Moskalenko, I. V., 1998, ApJ, 509, 212
- [27] Kamae, T., et al., 2006, ApJ, 647, 692
- [28] Aharonian, F., et al., 2009, A&A, 503, 817
- [29] Zhang, J.-L., Bi, X.-J. & Hu, H.-B., 2006, A&A, 449, 641
- [30] Moskalenko, I. V., Porter, T. A. & Strong, A. W., 2006, ApJ, 640, 155
- [31] Aharonian, F. & Neronov, A., ApJ, 2005, 619, 306
- [32] Ginzburg, V. L., & Ptuskin, V. S., 1981, ICRC, 2, 336
- [33] Drury, L, O'C., 1983, Rep., Prog., Phys., 46, 973
- [34] Heavens, A., F., 1984, MNRAS, 207, 1
- [35] Melia, F. & Falcke, H., 2001, ARA&A, 39, 309